Physics Letters A 375 (2011) 1980–1985

Contents lists available at ScienceDirect

Physics Letters A

www.elsevier.com/locate/pla

Stability of impulsively-driven natural convection with unsteady base state: implications of an adiabatic boundary

Christian F. Ihle [a,*], Yarko Niño [b]

[a] Program in Fluid Dynamics, Universidad de Chile, Av. Blanco Encalada 2002, 3rd floor, Santiago, Chile
[b] Department of Civil Engineering, Universidad de Chile, Av. Blanco Encalada 2002, 3rd floor, Santiago, Chile

ARTICLE INFO

Article history:
Received 15 January 2011
Accepted 14 March 2011
Available online 29 March 2011
Communicated by F. Porcelli

ABSTRACT

Stability conditions of a quiescent, horizontally infinite fluid layer with adiabatic bottom subject to sudden cooling from above are studied. Here, at difference from Rayleigh–Bénard convection, the temperature base state is never steady. Instability limits are studied using linear analysis while stability is analyzed using the energy method. Critical stability curves in terms of Rayleigh numbers and convection onset times were obtained for several kinematic boundary conditions. Stability curves resulting from energy and linear approaches exhibit the same temporal growth rate for large values of time, suggesting a bound for the temporal asymptotic behavior of the energy method.

1. Introduction

The onset of Rayleigh–Bénard convection in a horizontally infinite Boussinesq fluid layer of height d, subject to a vertical temperature difference, depends solely on the opposing effects of buoyancy and viscous forces in a time scale commensurate to that of temperature diffusion through the whole layer depth. Such balance is commonly expressed in dimensionless form using the Rayleigh number, $R = g\beta\Delta T\, d^3\nu^{-1}\kappa^{-1}$ [1,2], where g is the magnitude of the gravity acceleration vector, β, ν and κ are the coefficient of thermal expansion, kinematic viscosity and thermal diffusivity of the fluid respectively, and $\Delta T > 0$ is the characteristic vertical temperature difference. If the temperature profile that conforms the base state to perturbations is unsteady, time appears through the temperature evolution as a second variable that can play a role on the onset of convection. This sort of problem, referred to herein as URB, resembles many flows found in industry as well as in nature, which makes research on thermal convection to remain attractive, in terms of its application to practical problems, despite its long tradition. Examples can be found in industry [3] as well as in nature [4,5].

In the case of URB, the prediction of onset times for convection have been studied in the past by several authors using "frozen time" approaches, which correspond to an analogy of Rayleigh's analysis, considering time in the base state as a parameter and an exponential growth for disturbances. Alternatively, eigenfunction expansions of the temporal evolution of disturbances can be used to relax the, mathematically non-rigorous, separability assumption imposed upon the linear stability equation that is inherent to frozen time models. Such approach is known as the "amplification model" (see [6,7] and references therein for excellent reviews). The overall effect of unsteady heating have been estimated both using a frozen time model [8] and the energy method [6,9], the latter being a non-linear approach based upon an energy criterion for stability. This method has shown that the manner of heating positively affects global stability conditions: in particular, fast heating rates tend to make the system less stable [10,11], while the same conclusion have been obtained using an earlier, quasi-static approach [12].

A different and more recent method to predict onset times for convection is propagation theory [13], a linear analysis technique that relies on the assumption that temperature and velocity disturbances mainly develop in a length scale commensurate with that of the advancing base state temperature front. It is applicable when the temperature base state admits a similarity solution, allowing time to be implicitly included in a system of similarity linear disturbance equations, posing an eigenvalue problem in this new framework. This approach does not impose exponential growth rates for disturbances. A consequence of such relaxation is that, at difference with frozen time models, results depend on the Prandtl number ν/κ. Propagation theory have been used in a variety of problems involving different step and time-dependent boundary conditions for URB. A key result of such analyses is that theoretical times for the onset of convection have been found to be lower, by a factor of 1/4, than onset times detected experimentally (e.g., [13–17]), and close to such factor when heating binary mixtures, where the Soret effect conditionally induce convection [18], except when shear-free boundaries and a temperature step are imposed, where a factor of 1/10 is likely to fit better the data [19]. Studying the onset of convection in porous media, Riaz

* Corresponding author. Tel.: +562 6968400; fax: +562 6894171.
E-mail address: cihle@ing.uchile.cl (C.F. Ihle).

0375-9601/$ – see front matter
doi:10.1016/j.physleta.2011.03.027

et al. [20] considered the combination of a similarity space for disturbances (e.g., [13]), combined with an ad-hoc eigenfunction expansion [21,22], to find onset time predictions largely independent of the initial conditions, thus improving a major drawback of the amplification model. Although the recently developed methodologies mentioned have been proved to yield good results in the prediction of onset times for highly supercritical systems, for which it is reasonable that layers behave as if they were semi-infinite and often similarity solutions for the temperature base state can be found, they give no information about the effect of the manner of heating in overall stability conditions of URB, where frozen time and energy approaches are applicable.

A similar problem to that posed in URB is the flow that results from imposing a temperature step on one side of the horizontally infinite fluid layer without letting heat flow through the opposite boundary. The study of the stability of this kind of system is the matter of the present paper. This configuration resembles that of non-penetrative convection [23], and for convenience, the acronym NPC will be used hereafter to refer to it. A key feature of NPC is that the base state never reaches a non-zero steady state, and hence there is not a straightforward steady counterpart to compare critical Rayleigh numbers with, as in the case of URB. For this system and high Rayleigh numbers, propagation theory has been used to predict onset times for convection [19], where it was proved that the outer, adiabatic boundary has no effect on convection onset times. On the contrary, this is not necessarily true for Rayleigh numbers slightly larger than critical ones, which is discussed in detail in this Letter. Critical Rayleigh numbers for the onset of NPC have not been reported so far in the open literature. In the present paper, theoretical estimations of such values are proposed in the light of a frozen time model and the energy method, using several different kinematic boundary conditions. The energy method yields rigorous bounds for the stability of unsteady evolving systems. Studying the onset of convection, it has been used in the study of URB global stability [6,10,11,24], the effect of the Prandtl numbers on the onset of convection relaxing stability equations [25], and to determine reliable critical motion onset times and Marangoni numbers for evaporating droplets [26]. It is shown here that instability onset times predicted using the frozen time method are consistent and close to those computed using the energy method. Limits for this behavior are proposed by analyzing results for large values of time.

2. Problem description

The system is an initially quiescent, horizontally infinite Boussinesq fluid layer of height d, at a constant temperature $T_{\max}$, subject to a sudden temperature drop $\Delta T_{\mathrm{NPC}} = T_{\max} - T_{\min}$ on its upper surface, while the bottom is kept adiabatic. This imposes a transient evolution of the temperature field, which can be merely conductive on the whole domain of time, or driven by the combined effects of conduction and natural convection from a certain time on, provided a minimum imbalance between viscous and buoyant forces exists. Scales for disturbances are d, d^2/κ, κ/d and ΔT_{NPC} for length, time, velocity and temperature, respectively. Notation for dimensionless variables is as follows: x, y denote horizontal coordinates, z denotes a vertical upwards coordinate with origin at the bottom boundary, u, v and w denote disturbance velocity components in the x, y and z directions, respectively, and $\bar{\theta} = (T - T_{\min})/\Delta T_{\mathrm{NPC}}$ is the base state normalized temperature (from now on denoted simply temperature). In the case of the energy method equations, $\mathbf{v} = (u, v, w)^{\mathrm{T}}$ and θ stand for the disturbance dimensionless velocity and temperature, whilst in the frozen time model, $\hat{\mathbf{v}} = (\hat{u}, \hat{v}, \hat{w})^{\mathrm{T}}$ and $\hat{\theta}$ are their analogue definitions.

A Rayleigh number depending on the temperature step ΔT_{NPC} is defined as

$$Ra = \frac{g\beta \Delta T_{\mathrm{NPC}} d^3}{\nu\kappa}. \tag{1}$$

In NPC, in contrast with URB, since the bottom temperature is not fixed, the top and bottom temperature difference is a function of time. Therefore, the analogue to the top-bottom Rayleigh number definition in URB, R (as defined in Section 1), is time-dependent. As $\bar{\theta}(z=0,t) = (T_{\mathrm{bottom}} - T_{\min})/(T_{\max} - T_{\min}) = (T_{\mathrm{bottom}} - T_{\mathrm{top}})/\Delta T_{\mathrm{NPC}}$, it follows that a Rayleigh number in NPC based on the top and bottom temperatures can be expressed in terms of $\bar{\theta}$ and Ra as a modified Rayleigh number, $R_m = Ra\,\bar{\theta}(z=0,t)$. This parameter will be used to compare URB and NPC stability results. For instance, defining a URB constant top-bottom temperature difference numerically equal to ΔT_{NPC}, identifying $T_{\mathrm{bottom,URB}} = T_{\mathrm{max,NPC}}$ and $T_{\mathrm{top,URB}} = T_{\mathrm{min,NPC}}$, then $R_m = Ra\,\bar{\theta}(z=0,t) \leqslant Ra = R$, for any fixed value of t, given the same fluid properties, temperature difference and layer depth for URB and NPC problems. Although the control parameters Ra and R can be set to be equal, as in the previous example, this does not mean that the instability conditions associated with URB and NPC problems are the same. In fact, it is shown in this Letter that eigenvalues of the respective stability equations are generally different, which in the context of the above example means that the initial temperature step required for the onset of convection in NPC and URB problems can be expected to be different for identical fluid properties and layer thickness.

3. Non-linear stability analysis

Limiting conditions for the global stability of NPC are analyzed using the energy method. Details about the derivation of equations for this method are given elsewhere [9,27], so only some aspects concerning the interest of the present analysis are mentioned here. This approach relies on the definition of an energy functional, based upon a linear combination of kinematic and thermal components: $E = \langle |\mathbf{v}|^2/Pr + \lambda\, Ra\,\theta^2 \rangle$, where $\langle\cdot\rangle$ denotes integration over the fluid volume, with $\lambda > 0$ a coupling parameter.

According to energy theory, NPC convective motion can exist for a certain $t \geqslant t^*$ [28] if $Ra \geqslant Ra^*$ (where $Ra^* = Ra(t^*)$ is the analogy of the critical Rayleigh number found in the Rayleigh–Bénard stability problem with steady base state), provided disturbances exist from the beginning of the base state evolution. Following Homsy [6], defining $\phi = (\lambda Ra)^{1/2}\theta$, a set of Euler–Lagrange equations can be deduced:

$$\frac{1}{2}\rho_\lambda\left(\frac{1}{\sqrt{\lambda}} - \sqrt{\lambda}\frac{\partial\bar{\theta}}{\partial z}\right)\nabla_h^2\phi + \nabla^4 w = 0, \tag{2a}$$

$$\nabla^2\phi + \frac{1}{2}\rho_\lambda\left(\frac{1}{\sqrt{\lambda}} - \sqrt{\lambda}\frac{\partial\bar{\theta}}{\partial z}\right)w = 0. \tag{2b}$$

Here, ∇^{2n} is the Laplacian operator applied n times and ∇_h^2 its horizontal version.

Initially, the system remains quiescent and $\bar{\theta}(t \leqslant 0, z) = 1$. For $t > 0$, $\partial\bar{\theta}/\partial z = \partial\phi/\partial z = w = 0$ at $z = 0$, $\bar{\theta} = \phi = w = 0$ at $z = 1$; besides, $\partial w/\partial z = 0$ is imposed on a rigid boundary and $\partial^2 w/\partial z^2 = 0$ on a free one (both types or kinematic boundary conditions are applied alternatively to top and bottom surfaces). ρ_λ is a Lagrange multiplier which is a solution of the problem:

$$\frac{1}{\rho_\lambda} = \max_h\left\{\frac{\langle w\phi\rangle}{\sqrt{\lambda}} - \sqrt{\lambda}\left\langle w\phi\frac{\partial\bar{\theta}}{\partial z}\right\rangle\right\}, \tag{3a}$$

$$\left\langle \nabla\mathbf{v} : \nabla\mathbf{v} + |\nabla\phi|^2 \right\rangle = 1, \tag{3b}$$

Table 1
Critical overall stability bounds $(t^*, Ra^* = Ra(t^*))$ and their corresponding optimal wavenumbers α^* for NPC, obtained with the energy method (labeled as EM, in columns 2 to 5), and frozen time model (labeled as FTM, in columns 6 to 9), for different kinematic boundary conditions. $R_m^* = Ra(t^*)\bar{\theta}(z=0,t^*)$. In the first column, the first kinematic condition corresponds to the upper boundary, which is cooled in every case, while the second one corresponds to the bottom boundary.

Condition	EM				FTM			
	t^*	α^*	Ra^*	R_m^*	t^*	α^*	Ra^*	R_m^*
Rigid–rigid	0.101	2.65	1 438.6	1 363.6	0.105	2.64	1 463.1	1 378
Free–rigid	0.087	2.28	825.4	798.1	0.092	2.27	840	806.8
Rigid–free	0.114	2.16	865.8	803.1	0.117	2.15	882.1	813.8
Free–free	0.103	1.8	452.4	427.4	0.106	1.79	460.6	433.1

where h is a function space that allows solutions for non-linear disturbance velocity $\mathbf{v}$ and temperature θ (and hence ϕ) such that they satisfy prescribed kinematic and thermal boundary conditions, as well as $\nabla\cdot\mathbf{v}=0$ (see [6] and references therein for a more complete discussion). Noting that (2) can be decomposed into horizontal Fourier modes, if α is the dimensionless wavenumber of a horizontal wavevector and ρ_λ is the lowest eigenvalue of (2) with appropriate boundary conditions, the goal is to find an optimal solution:

$$\tilde{\rho} = \max_{\lambda}\min_{\alpha}\rho_\lambda. \tag{4}$$

The term $\partial\bar{\theta}/\partial z$ is time-dependent, and so then is $\tilde{\rho}$. If the flow is strongly stable, i.e., if the energy decreases exponentially with time for arbitrary amplitude disturbances, then $\rho_\lambda > \sqrt{Ra}$ [27]. This corresponds to the decreasing portion of the $\tilde{\rho}(t)$ curve that results from the solution of the problem (4) for different values of time [6]. The fluid layer will be globally stable for $\sqrt{Ra} < \min_t \tilde{\rho}$.

Since λ is chosen to yield the largest eigenvalue of (2), it can also be a function of time, but system (2) is obtained under the assumption that λ is a constant. Generally, this is not a major obstacle for the analysis, as Homsy [6] showed that the derivation just outlined still holds if $\mathrm{d}\lambda/\mathrm{d}t < 0$, and that, when ρ_λ^2 varies monotonically with time, the optimal lower bound for stability does not change if $\mathrm{d}\lambda/\mathrm{d}t \geqslant 0$. In the present case, for each of the kinematic boundary conditions imposed, corresponding minimum is achieved from monotonic curves $\rho(t)$, and consequently, computed optimal lower bounds are considered to be sound.

The shooting method and an optimization routine based on the Newton–Raphson iteration, whose validation has been previously reported [19], were used to solve the minimax problem (4). Time-dependent $\rho_\lambda(t)$ curves obtained for different boundary conditions are shown in Fig. 1. Stability results for NPC are summarized in Table 1.

To validate the present application of the energy method, the analysis of unsteady URB was chosen, since results of a previous application of such method to that system are available [11]. Critical stability parameters, i.e., minimum Rayleigh number, corresponding time and wavenumber, obtained with the energy method for the unsteady URB problem, are reported in Table 2, together with those obtained by Neitzel [11], with the exception of critical wavenumbers, which were not reported by him. Good general agreement between both sets of results was found. However, at difference with Neitzel's results, present computations show the existence of a subcritical minimum for the free–free condition. In the rest of the cases, correspondence among Ra^* values was found within the zero-decimal precision reported by Neitzel [11]. On the other hand, in every case, present results were observed to converge to the well-known steady-state Ra^* values as $t\to\infty$ [2].

4. Linear stability analysis

Limiting conditions for the instability of the NPC system are analyzed using the frozen time model. To derive the equations

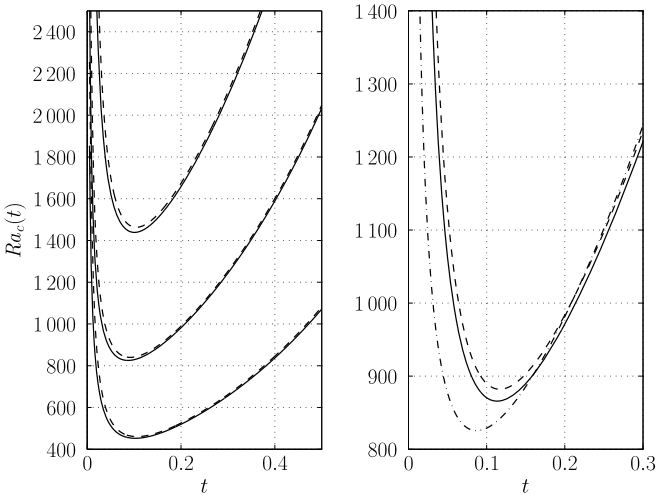

Fig. 1. Critical NPC stability curves for fixed values of time, obtained from the optimization problem using the energy method, corresponding to system (4) (solid lines), and frozen time model, corresponding to Eqs. (6) (dashed lines), respectively. Left panel: from top to bottom, curves corresponding to rigid–rigid, free–rigid and free–free kinematic boundary conditions, respectively. Right panel: curves corresponding to the rigid–free boundary condition. The dash-dotted line corresponds to the free–rigid critical curve computed using the energy method. The first kinematic condition applies to the top boundary.

Table 2
Critical overall stability bounds $(t^*, Ra^* = Ra(t^*))$ and their corresponding optimal wavenumbers α^* for URB using the energy method. Columns 5 and 6 show corresponding results by Neitzel [11]. The first kinematic condition corresponds to the upper boundary, which is cooled in every case, while the second one corresponds to the bottom boundary. When no critical time is given, curves decrease monotonically toward asymptotes in the (t, Ra) space.

Condition	Present algorithm			Neitzel [11]	
	t^*	α^*	Ra^*	t^*	Ra^*
Rigid–rigid	0.138	3.12	1699.4	0.14	1699
Free–rigid	–	2.68	1100.6	–	1101
Rigid–free	0.085	2.69	1012.9	0.08	1013
Free–free	0.135	2.23	654.6	–	657.5

for this method, it is argued that NPC onset corresponds with the transition between the purely conductive and the conductive-convective states of the system. As the former state is independent of the Prandtl number, it is expected that the instability condition should also be independent of this parameter. The z-component of the linearized momentum and energy disturbance equations in the present system are, respectively:

$$\left(\frac{1}{Pr}\frac{\partial}{\partial t} + \frac{\partial^2}{\partial z^2} - \alpha^2\right)\left(\frac{\partial^2}{\partial z^2} - \alpha^2\right)\hat{w} - \alpha^2\hat{\theta} = 0, \tag{5a}$$

$$\frac{\partial\hat{\theta}}{\partial t} + Ra\,\hat{w}\frac{\partial\bar{\theta}}{\partial z} - \left(\frac{\partial^2}{\partial z^2} - \alpha^2\right)\hat{\theta} = 0, \tag{5b}$$

where $\hat{\theta}(z,t)$ and $\hat{w}(z,t)$ are first order disturbances of temperature and vertical velocity, respectively. Here, α and boundary con-

ditions for disturbances have the same definition as in the energy approach.

In the frozen time model, time is treated as a parameter and hence solutions of the form $(\hat{\theta}, \hat{w}) = [\theta_1(z), w_1(z)] \exp \sigma t$ are considered. This assumption turns the PDE system (5) into an ODE system that corresponds to an eigenvalue problem, where the latter can be found in spite of the fact that system (5) is not separable. The validity of this quasi-static approach requires that disturbances evolve much faster than the base state conductive heat flow, represented by the term $\partial\bar{\theta}/\partial z$. This is generally the case in the present analysis as is discussed next. Indeed, in the case of impulsively-driven URB, it has been shown [8] that for supercritical systems (i.e., those with values of the Rayleigh number greater than the critical one for the onset of instabilities), growth rates of disturbances of frozen time model variations converge to those computed using transient analysis [21], where disturbances are written in terms of Fourier series with time-dependent coefficients, turning system (5) into an eigenvalue problem subject to certain initial conditions. In their problem, the temporal threshold of validity suggested by Gresho and Sani [8] is $t \sim 0.01$, such that for larger times the frozen time model would yield similar results as the transient analysis. Following the trend of this result, in the NPC system the quasi-static hypothesis is likely to be reasonable, as in the present analysis estimated values of the onset time of instabilities are on the order of 0.1. These values are computed from marginal stability curves, obtained by solving the optimization problem $\min_{\alpha,t} Ra$, where

$$\left(\frac{\sigma}{Pr} + \alpha^2 - \mathrm{D}^2\right)\left(\mathrm{D}^2 - \alpha^2\right) w_1 + \alpha^2 \theta_1 = 0, \tag{6a}$$

$$\sigma\theta_1 + Ra\, w_1 \frac{\partial\bar{\theta}}{\partial z} - \left(\mathrm{D}^2 - \alpha^2\right)\theta_1 = 0, \tag{6b}$$

$$\sigma = 0, \tag{6c}$$

with $\mathrm{D}(\cdot) \equiv \mathrm{d}(\cdot)/\mathrm{d}z$. The marginal stability curves obtained are shown in Fig. 1. Onset times, corresponding to the minima of these curves, are indeed of about 0.1. The marginal stability curves appear to be physically meaningful compared with global stability curves obtained with the energy method, as critical Rayleigh numbers and corresponding times are greater and lower, respectively, than those predicted by the energy theory. Nonetheless, although present results are thought to describe well the physics underlying the present problem, further verification with Foster's approach [21], which is beyond the scope of the present Letter, would give additional information about this point.

The present numerical algorithm, used for both the linear and non-linear analyses reported in this Letter, was also checked in the context of the frozen time model, using results of Gresho and Sani [8] in the case of unsteady URB. In the rigid–rigid case, the present analysis yields a minimum of $Ra = 1\,706.41$ at $t = 0.185$, whereas for the same case, Gresho and Sani [8] computed $Ra = 1\,706.36$ and $t = 0.186$, respectively.

5. Discussion

For small enough values of dimensionless time, when the thermal penetration depth is small compared with the thickness of the fluid layer, the effect of temperature and velocity disturbances is slight in contrast with the rapid evolution of the temperature base state. As a matter of fact, in the light of both of the approaches considered, in this time range the system exhibits critical Rayleigh numbers that are increasingly high as time decreases. On the other hand, in this time range, URB and NPC have the same instability behavior as they are independent of the boundary opposite to the step change in temperature [19]. Writing a force balance taking into account the effects of viscosity, thermal diffusivity and buoyancy, it can be shown that $Ra_c \sim t^{-3/2}$ (see also [29]). The validity of this relation relies on the assumption that the thermal boundary layer thickness scales with $\sqrt{t}$, which is true if $t \lessapprox 0.01$. If the dimensionless time is not so small, then the latter scaling is not valid, and the temporal behavior of the stability (as well as instability) of the system saturates to a minimum value of the Rayleigh number, which depends on kinematic boundary conditions on both sides, as shown in Table 1. In the present system, for larger values of time, the available heat from which an instability can give rise to thermal convection decays exponentially to zero with time. As it will be shown later, a consequence of this is that corresponding critical Rayleigh numbers must necessarily increase exponentially as time increases, at difference with URB where convergence to the steady-state stability limit is obtained.

Data on Table 1 indicate that the NPC system becomes unstable before and at lower Rayleigh numbers than URB given the same kinematic boundary conditions. Previously, Joseph and Shir [30] commented on the destabilizing effect of the Robin boundary condition (i.e., a generalization of that applied in the NPC problem, consisting of an isothermal boundary condition at one boundary and a heat flux boundary condition at the other), showing via manipulations of the set of energy Euler–Lagrange equations that the corresponding stability limit is a monotonically increasing function of the Nusselt number (Nu) on the boundaries. In particular, given kinematic boundary conditions, fixing the upper thermal boundary condition as isothermal and allowing the prescribed heat flux on the bottom to be set through Nu, according to Joseph and Shir [30], the lowest stability boundary will be found for $Nu = 0$, that is, for the NPC setup. The lack of heat flow on the bottom precludes compensation of the buoyant force exerted downwards to fluid parcels due to the cooling on top by other volume forces from the bottom, such as the upwelling force that exists in the URB case, caused by the heating at $z = 0$. Therefore, the numerical results found in the light of the energy method are consistent with present and previous predictions for URB and also thought to be physically appealing.

Experimental data for the minimum Rayleigh number necessary for NPC are available only for the rigid–rigid case [31], for which a critical time-dependent condition of $R_m = 1\,700$ was found. This is consistent with the theoretical R_m lower bound reported here, equal to 1 363.6 (Table 1).

The relationship between critical or onset times predicted by the energy method (i.e., times that minimize the energy functional) in NPC and URB depends on upper and lower boundary conditions. According to results shown in Tables 1 and 2, dimensionless onset times in NPC (0.101 and 0.103) are lower than those in URB (0.138 and 0.135) for rigid–rigid and free–free cases, respectively. The opposite is true in the rigid–free case, with onset times of 0.114 and 0.085 for NPC and URB, respectively. No comparison of critical times can be done in the free–rigid case, since in URB, monotonic convergence to the steady-state critical value was achieved, both in the present Letter and in Neitzel [11]. Regarding computed results for NPC using both approaches, it is readily apparent from Fig. 1 that, given fixed boundary conditions and values of time, linear and non-linear results are similar, being critical Rayleigh numbers yielded by the frozen time model always greater to those produced by the energy method, with relative differences on the order of 0.02.

Stability (and instability) curves corresponding to the free–rigid and rigid–free cases cross each other for times equal to 0.161 and 0.175 according with energy and frozen time computations, respectively (Fig. 1). In the free–rigid case, the system can experiment convective motion before and with a lower Rayleigh number than in the rigid–free system, due to the lack of restrictions for the generation of a horizontal flow on the top lid. As time

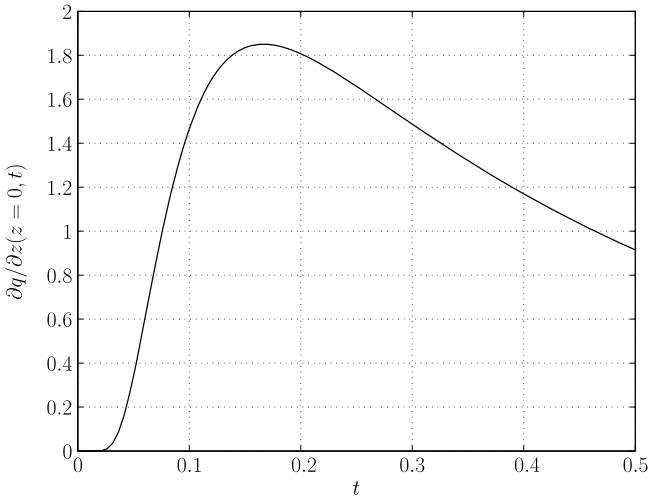

Fig. 2. Vertical gradient of the base heat flux at $z=0$, $\partial q/\partial z(z=0,t) = -\partial\bar{\theta}^2/\partial z^2(z=0,t)$. The maximum occurs at $t=0.167$.

goes on, the vertical heat flux space derivative near the bottom, $\partial q/\partial z(z=0,t) = -\partial\bar{\theta}^2/\partial z^2(z=0,t)$, departs from zero (Fig. 2), and an interplay between this evolution and the kinematic boundary condition sets in. It is interesting that the mentioned curve crossing occurs, according to both methods, very close to the maximum of $\partial q/\partial z(z=0,t)$, found at $t=0.167$. After this time, rigid–free curves dip slightly below free–rigid ones toward an asymptotic difference, to be analyzed below.

It can be argued whether the increasing portions of the set of marginal stability curves corresponding to Fig. 1 can be possibly reached experimentally. Although it is quite difficult to suppress experimentally every natural source of disturbance, which would be one way to retain the stability of the system after the critical onset time at a higher Rayleigh number than that corresponding with the global minimum, it may be possible to suppress convection through the use of active control systems (see, e.g., [32]), shifting critical Rayleigh numbers significantly [33]. Thus, the discussion of conditions for stability at large values of time is considered meaningful in physical terms.

It is noted that for large values of time, the base state vertical base heat flux can be approximated as:

$$\frac{\partial\bar{\theta}}{\partial z}(z, t\gg 0) \approx -2\sin\left(\frac{\pi z}{2}\right)\exp\left(-\frac{\pi^2}{4}t\right). \tag{7}$$

In particular, this is a very good approximation of $\partial\bar{\theta}/\partial z$ for $t \gtrapprox 0.4$.

Using the energy method, Joseph and Shir [30] have shown that the value of the coupling parameter, λ^*, that maximizes problem (4), thus making $\partial\rho_\lambda/\partial\lambda = 0$, satisfies $\lambda^* = -\langle w\phi\rangle/\langle w\phi(\partial\bar{\theta}/\partial z)\rangle$, where in the present case,

$$\lambda^* \approx \frac{\langle w\phi\rangle}{2\langle w\phi\sin(\pi z/2)\rangle}\exp\left(\frac{\pi^2}{4}t\right) \geqslant \frac{1}{2}\exp\left(\frac{\pi^2}{4}t\right), \tag{8}$$

showing that the critical coupling parameter has an exponential factor (with a dimensionless time constant equal to $4/\pi^2$) for large values of time. Although $w\phi$ is also a function of time, from numerical computations it is evident that the latter dependence vanishes for large enough dimensionless times (in the present case, on the order of 0.5). Computed prefactors $\langle w\phi\rangle/\langle 2w\phi\sin(\pi z/2)\rangle$, extrapolated for large values of time, are 0.76, 0.72, 0.85 and 0.8 for the rigid–rigid, free–rigid, rigid–free and free–free cases respectively. Critical Rayleigh numbers, $\rho^2_{\lambda^*}$, exhibit the same growth rate, as can be readily checked using (3a) for λ^* and (8). Corresponding

Table 3
Wavenumbers and prefactors for Rayleigh numbers, given by $Ra_\infty = Ra(t)\times\exp[-\pi^2 t/4]$, valid for large values of time ($t \gtrsim 0.5$), obtained with the energy method (labeled as EM, in columns 2 and 3), and frozen time model (labeled as FTM, in columns 4 and 5), for different kinematic boundary conditions.

Condition	EM		FTM	
	α_∞	Ra_∞	α_∞	Ra_∞
Rigid–rigid	2.61	995.9	2.61	1 004.4
Free–rigid	2.25	592	2.25	596.2
Rigid–free	2.14	580.8	2.13	587.5
Free–free	1.78	311.9	1.78	314.9

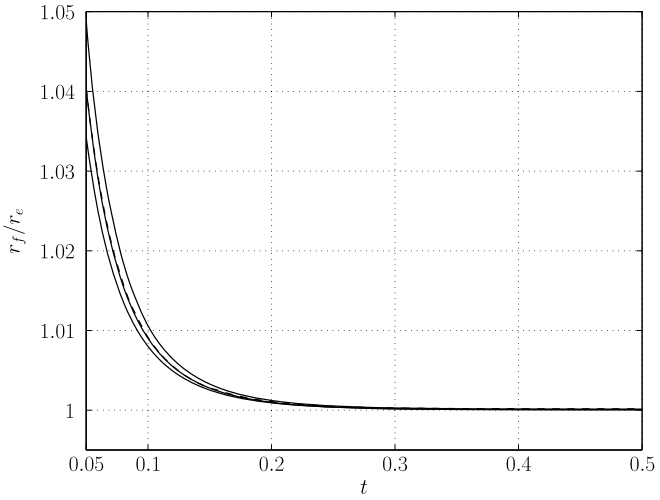

Fig. 3. Temporal evolution of the quotient r_f/r_e, where $r_f = Ra/Ra_\infty$ using the frozen time model and $r_e = Ra/Ra_\infty$ using the energy method (see Table 3 for corresponding values and definitions). Upper and lowermost curves represent the rigid–free and free–rigid cases, respectively. The dashed, central curve corresponds to the free–free case and the remaining one, the rigid–rigid condition. The first condition applies to the top boundary.

prefactors for such growth rate, Ra_∞, along with their corresponding wavenumbers, α_∞, are shown in Table 3.

In the case of the linearized equations, for large values of time, a temporal dependence of eigenvalues can be set to compensate the exponential decrease of the base state gradient. This can be achieved in the present case if $Ra(t) \sim \exp(\pi^2 t/4)$. Thus, system (5) is separable, and the assumption of an exponential growth of disturbances is mathematically consistent. Marginal condition for this case corresponds to $\sigma = 0$ [34], and equations turn to the following eigenvalue problem:

$$\left(\mathrm{D}^2 - \alpha_\infty^2\right)^2 w_1 - \alpha_\infty^2\theta_1 = 0, \tag{9a}$$

$$Ra_\infty w_1 f(z) - \left(\mathrm{D}^2 - \alpha_\infty^2\right)\theta_1 = 0, \tag{9b}$$

with $f(z) = -2\sin(\pi z/2)$. Results for the different boundary conditions considered are shown in Table 3, where it is observed that minimum differences between stability and instability are not asymptotically zero, though very small. As the frozen time model becomes progressively better with time, lack of convergence among energy and frozen time approaches, must be due to the bound limitation given by construction of the energy method. For values of dimensionless time greater than about 0.2, the difference between energy and frozen time critical Rayleigh values is nearly constant. Fig. 3 shows this trend, where the ratio r_f/r_e is plotted as a function of time, with $r_f = Ra/Ra_\infty$ using the frozen time model and $r_e = Ra/Ra_\infty$ using the energy method (see also Table 3). This result supports the validity of computations obtained with the frozen time model, as their difference with asymptotic

ones (which are more accurate for larger values of dimensionless time) are slight.

6. Conclusions

The onset of Rayleigh–Bénard convection depends on two aspects, namely, the relative importance of the overall temperature difference, fluid properties and layer depth and, on the other hand, the influence of the manner of heating both in time and in the existence of subcritical stability thresholds. The first topic has been covered early in the 20th century, while the latter more recently, motivated by the large number of applications in industry and environment. Related to this family of problems is that of the stability of an infinite Boussinesq fluid layer with one side kept adiabatic while the other is subject to a temperature step, labeled herein as NPC. Onset times for such system were recently studied with both theoretical and experimental approaches [19,35]. However, the basic question regarding the minimal control parameter values and maximal expected times to observe convective patterns remained unanswered. This Letter fills such gap.

Non-linear and linear stability analyses of NPC, obtained from the application of energy theory and the frozen time model, respectively, were presented and discussed in this Letter. Given the thermal boundary conditions imposed, the base state of the system is unsteady on the whole domain of time. Overall stability and instability thresholds, expressed in terms of critical onset times and Rayleigh numbers, were presented for different kinematic boundary conditions, including rigid or free top and bottom surfaces. The marginal stability curves obtained from both linear and non-linear approaches are very close to each other and considered to be physically meaningful, as critical Rayleigh numbers and corresponding times obtained with the frozen time model (representing the instability limit) are greater and lower, respectively, than those predicted by the energy theory (representing the stability limit). Results show that the present system becomes unstable before and with lower Rayleigh numbers than Rayleigh–Bénard convection, in agreement with previous theoretical findings for the type of thermal boundary conditions associated with both systems. Critical stability curves (i.e., critical Rayleigh number versus time) for free–rigid and rigid–free cases exhibit a crossing point, according to both linear and non-linear approaches. It is suggested that such crossing represents a transitional stage at which the influence of the bottom boundary becomes stronger than that of the top one, on the balance between stabilizing and destabilizing effects. Using both the energy method and the frozen time model, the latter was found to occur near the maximum value of the gradient of the base state vertical heat flux at the bottom of the fluid layer. At difference with unsteady Rayleigh–Bénard convection, an exponential growth of eigenvalues was found at large values of time, using both the energy method and the frozen time model. In both cases, the time constant for such growth is the same. However, prefactors do not converge, but slightly and consistently differ. Since as time increases the frozen time approach becomes increasingly more accurate, this result suggests a bound for the temporal asymptotic accuracy of the non-linear energy method.

Acknowledgements

The authors gratefully acknowledge support from the Chilean National Commission for Scientific and Technological Research, CONICYT, the Department of Civil Engineering of the University of Chile, and Fondecyt Project No. 1040494.

References

[1] Lord Rayleigh, Philos. Mag. 32 (1916) 529.
[2] P.G. Drazin, W.H. Reid, Hydrodynamic Stability, Cambridge University Press, 1981.
[3] R.C. Kerr, A.W. Woods, M.G. Worster, H.E. Huppert, Nature 340 (6232) (1989) 357.
[4] P.F. Linden, Perspectives in Fluid Dynamics: A Collective Introduction to Current Research, Cambridge University Press, 2001, chap. 6, pp. 289–345.
[5] T. Jonas, A. Stips, W. Eugster, A. Wüest, J. Geophys. Res. 108 (2003) 26/1.
[6] G.M. Homsy, J. Fluid Mech. 60 (1973) 129.
[7] R.J. Goldstein, R.J. Volino, J. Heat Transfer - Trans. ASME 117 (1995) 808.
[8] P.M. Gresho, R.L. Sani, Int. J. Heat Mass Transfer 14 (1971) 207.
[9] D.D. Joseph, Arch. Rat. Mech. Anal. 22 (1966) 163.
[10] P.C. Wankat, G.M. Homsy, Phys. Fluids 20 (1977) 1200.
[11] G.P. Neitzel, Phys. Fluids 25 (1982) 210.
[12] I.G. Currie, J. Fluid Mech. 29 (1967) 337.
[13] D.J. Yang, C.K. Choi, Phys. Fluids 14 (2002) 930.
[14] M.C. Kim, H.K. Park, C.K. Choi, Theoret. Comput. Fluid Dyn. 16 (2002) 49.
[15] C.K. Choi, J.H. Park, M.C. Kim, J.D. Lee, J.J. Kim, E.J. Davis, Int. J. Heat Mass Transfer 47 (19–20) (2004) 4377.
[16] C.K. Choi, J.H. Park, M.C. Kim, Heat Mass Transfer 41 (2004) 155.
[17] M.C. Kim, J.H. Park, C.K. Choi, Chem. Eng. Sci. 60 (19) (2005) 5363.
[18] M.C. Kim, C.K. Choi, J.-K. Yeo, Phys. Fluids 19 (8) (2007) 084103.
[19] C.F. Ihle, Y. Niño, Int. J. Heat Mass Transfer 49 (2006) 1442.
[20] A. Riaz, M. Hesse, H.A. Tchelepi, F.M. Orr Jr., J. Fluid Mech. 548 (2006) 87.
[21] T.D. Foster, Phys. Fluids 8 (1965) 1770.
[22] J.L. Robinson, Phys. Fluids 19 (1976) 778.
[23] R.J. Adrian, R.T.D.S. Ferreira, T. Boberg, Exp. Fluids 4 (1986) 121.
[24] J. Ennis-King, I. Preston, L. Paterson, Phys. Fluids 17 (2005) 084107.
[25] M.C. Kim, C.K. Choi, D.Y. Yoon, Phys. Lett. A 372 (2008) 4709.
[26] V.M. Ha, C.L. Lai, Int. J. Heat Mass Transfer 47 (2004) 3811.
[27] D.D. Joseph, Arch. Rat. Mech. Anal. 20 (1) (1965) 59.
[28] R.J. Gumerman, G.M. Homsy, J. Fluid Mech. 68 (1975) 191.
[29] B.S. Jhaveri, G.M. Homsy, J. Fluid Mech. 114 (1982) 251.
[30] D.D. Joseph, J. Fluid Mech. 26 (1966) 753.
[31] R.K. Soberman, Phys. Fluids 2 (2) (1959) 131.
[32] L.E. Howle, Phys. Fluids 9 (7) (1997) 1861.
[33] J. Tang, H.H. Bau, Phys. Rev. Lett. 70 (1993) 1795.
[34] A. Pellew, R.V. Southwell, Proc. Roy. Soc. A 176 (966) (1940) 312.
[35] C.F. Ihle, Y. Niño, Onset of modulated penetrative convection: A theoretical and experimental analysis, in: Proceedings of the Sixth International Symposium on Stratified Flows, vol. 1, Perth, Australia, 2006, pp. 557–562.